

# Motion Planning Explorer: Visualizing Local Minima using a Local-Minima Tree

Andreas Orthey, Benjamin Frész, Marc Toussaint

**Abstract**—We present an algorithm to visualize local minima in a motion planning problem, which we call the motion planning explorer. The input to the explorer is a planning problem, a sequence of lower-dimensional projections of the configuration space, a cost functional and an optimization method. The output is a local-minima tree, which is interactively grown based on user input. The local-minima tree captures non-self-intersecting local minima of a problem. We show the motion planning explorer to faithfully capture the structure of four real-world scenarios.

**Index Terms**—Visualization in Motion Planning, Interactive Motion Planning, Topological Motion Planning

## I. INTRODUCTION

In motion planning, we develop algorithms to move robots from an initial configuration to a desired goal configuration. Such algorithms are essential for manufacturing, autonomous flight, computer animation or protein folding [14].

Most motion planning algorithms are black-box algorithms<sup>1</sup>. A user inputs a goal configuration and the algorithm returns a motion. In real-world scenarios, however, black-box algorithms are problematic. Human users cannot interact with the algorithm. There is no way to guide or prevent motions. Human users cannot visualize the internal mechanism of the algorithm. There is no intuitive way to understand or debug the algorithm. Human users cannot predict the outcome of the algorithm. There is no way for coworkers to avoid or plan around a robot. Black-box algorithms are therefore an obstacle for having robots move in a safe, predictable and controllable way.

In an effort to make robotic algorithms visualizable, predictable and interactive, we develop the motion planning explorer. Using the planning explorer, we enumerate and visualize local minima. We define a local minimum as *a path which is invariant under minimization of a cost functional*. To each local minimum we can associate an equivalence class, the equivalence class of all paths converging to the local minimum.

Using this equivalence relation, we utilize a fiber bundle construction — a sequence of admissible lower-dimensional projections [20] — to organize the local-minima into a tree. Since the number of leaves of this tree is usually countable infinite, we do not compute the tree explicitly, but let human users interactively explore the tree.

The authors are with the University of Stuttgart, Germany (e-mail: {andreas.orthy, marc.toussaint}@ipvs.uni-stuttgart.de)

<sup>1</sup>We call an algorithm a black-box algorithm whenever the internal mechanism is hidden from the user. [1]

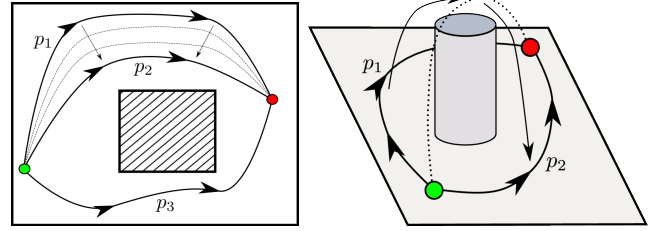


Fig. 1: **Left:** Homotopic paths in 2D. **Right:** Distinct local minima which are homotopic in 3D.

This local-minima tree is primarily a tool to visualize the problem structure. However, we believe it to be more widely applicable. The tree is a visual guide to the (topological) complexity of the problem [26]. The tree visualizes where a deformation algorithm [29] converges to. The tree allows us to interact with the algorithm, useful for factory workers guiding their robot or the control of computer avatars. The tree can be used to give high-level instructions to a robot — crucial when bandwidth is limited. The tree provides alternatives for efficient replanning [5]. Finally, the tree can be a source of symbolic representations [28].

### A. Contributions

We make three original contributions

- 1) We propose a new datastructure, the local-minima tree, to enumerate and organize local minima
- 2) We propose an algorithm, the motion planning explorer, which creates a local-minima tree from input by a human user
- 3) We demonstrate the performance of the motion planning explorer on realistic planning problems and on pathological environments

## II. RELATED WORK

We can visualize a motion planning problem by visualizing its decomposition. However, there is no clear consensus among researchers on the notion of decomposition.

Often the problem is decomposed topologically [7]. In a topological decomposition, we partition the pathspace into homotopy classes, sets of paths continuously deformable into each other [17] (See Fig. 1 Left). We can compute homotopy classes by computing an H-signature of paths [4] measuring the times a path crosses lines emanating from obstacles. This can be generalized to higher dimensions, where we measure how often a path passes through holes

in configuration space [3]. We can also compute homotopy classes by approximating the free configuration space by a simplicial complex [23], a generalization of triangulations to higher dimensions, and then use the simplicial complex to check if two paths are homotopic.

Topological decompositions, however, do not adequately capture the intricate geometry of configuration space constraints and are often computationally inefficient. Many alternative definitions have been proposed to obtain computationally-efficient homotopy-like decompositions. Examples include digital homotopy relations [25],  $K$ -order deformability [11] and convertibility of paths [19].

However, computationally-efficient homotopy decompositions fail to give a proper pathspace partitioning. All previously named efficient decompositions are violating the transitivity relation<sup>2</sup> and do not constitute an equivalence relation. This makes it difficult to have clear lines of demarcation between path subsets. It is also unclear how to visualize overlapping path sets.

We believe a more appropriate decomposition is the cost-function decomposition. In a cost-function decomposition, we group paths together whenever *they converge under optimization to the same local minimum*. With such an approach, we can leverage optimization methods for computational efficiency and compute partitions of the pathspace.

The computation of local minima of cost functions belongs to the topic of optimal motion planning [13]. In optimal motion planning we like to find the global cost-function minimum. Recently, several sampling-based algorithms have been proposed which are asymptotically optimal, i.e. we will find the global optimum if time goes to infinity [13]. Recent extensions of those algorithms exploit graph sparsity [6], improve upon convergence time [12] and solve kinodynamic problems [16].

However, most optimal planning algorithms will find only the global optimal path, but not necessarily all local optimal paths. Our work differs by computing all local minima and arranging them in a local-minima tree. We rely on computations of optimal sparse graph structures [6] and on fiber bundle projections [20].

Our tree of local minima can be seen as a hierarchical clustering of paths. A similar approach to hierarchical clustering is based on the Frechét distance [10], which is defined as the best reparameterization of two paths minimizing Euclidean distance between points along the reparameterization. This approach, however, is not interactive and agglomerative (bottom-up).

We instead use a divisive (top-down) approach, which is interactive. Interactive methods in motion planning have been used together with user drawings of paths [24]. Such an approach, however, is not intuitive in higher-dimensional spaces. We instead provide options to a user in form of lower-dimensional local minima.

<sup>2</sup>Transitivity holds for a pathspace decomposition if whenever a path  $a$  is equivalent to a path  $b$ , and  $b$  is equivalent to a path  $c$ , then  $a$  is equivalent to  $c$ .

### III. BACKGROUND

Let  $(X, \phi)$  be the *planning space*, consisting of the configuration space  $X$  of a robot and the *constraint function*  $\phi : X \rightarrow \{0, 1\}$  which on input  $x \in X$  outputs zero when  $x$  is constraint-free and one otherwise. We extend  $\phi$  such that on input of subsets  $U \subseteq X$  outputs zero when at least one  $x \in U$  is constraint-free and to one otherwise. The constraint function defines the *free configuration space*  $X_f = \{x \in X \mid \phi(x) = 0\}$ . Given an initial configuration  $x_I \in X_f$  and a goal configuration  $x_G \in X_f$ , we are interested in finding a path in  $X_f$  connecting them. We call  $(X_f, x_I, x_G)$  a *motion planning problem* [20].

The space of solutions to a planning problem is given by its *path space*. The path space  $P$  is the set of continuous paths  $\mathbf{p} : I \rightarrow X_f$  from  $I = [0, 1]$  to  $X_f$  such that  $\mathbf{p}(0) = x_I$  and  $\mathbf{p}(1) = x_G$ . We equip the pathspace  $P$  with a cost functional  $c : P \rightarrow \mathbb{R}_{\geq 0}$  on  $P$ . Examples of cost functionals are minimum-length, minimum-energy, or maximum-clearance.

#### A. Admissible Fiber Bundles

We can often simplify planning spaces using *fiber bundles* [20]. A fiber bundle is a tuple  $(X, Y, \pi, \pi_\phi)$  consisting of a mapping

$$\pi : X \rightarrow Y \quad (1)$$

which maps open sets to open sets and a mapping  $\pi_\phi : \phi \rightarrow \phi_Y$ , which map a planning space  $(X, \phi)$  to a lower-dimensional space  $(Y, \phi_Y)$ . We say that  $\pi_\phi$  is *admissible* if the admissibility condition  $\phi_Y(y) \leq \phi(\pi^{-1}(y))$  holds for all  $y \in Y$ , whereby we call  $\pi^{-1}(y)$  the *fiber* of  $y$  in  $X$ . We then call  $\pi$  an admissible lower-dimensional projection,  $X$  the bundle space, and  $Y$  the *quotient-space* of  $X$  under  $\pi$  [15].

Often it is advantageous to define chains of  $K$  fiber bundles  $(X_k, X_{k-1}, \pi_k, \pi_{\phi_k})$  with admissible mappings

$$\{\pi_k : X_k \rightarrow X_{k-1}\}_{k=1}^K \quad (2)$$

such that  $X_K = X$  and the constraint functions are admissible such that  $\phi_{k-1}(x_{k-1}) \leq \phi_k(\pi_k^{-1}(x_{k-1}))$  for all  $x_{k-1} \in X_{k-1}$ . Admissible fiber bundles have been shown to be a generalization of constraint relaxation, a source of admissible heuristic and can reduce planning time by up to one order of magnitude [20].

There are multiple ways simplifying a configuration space to construct a fiber bundle. We can often construct simpler robotic system by removing constraints, through nesting lower-dof robots [21], removing links [2] or shrinking obstacles [8].

If the projection mappings  $\pi$  and  $\pi_\phi$  are obvious from the context, we will often denote the fiber bundle simply as  $X \rightarrow Y$ . As an example, we write  $SE(2) \rightarrow \mathbb{R}^2$  for the car in Fig. 2, whereby we mean that the car has been simplified by a nested disk. The nested disk is an abstraction of the car, removing the orientation. The mapping  $\pi$  in that case maps position and orientation onto position, and  $\phi_{\mathbb{R}^2}$  is zero whenever the disk is collision-free.

#### IV. METHOD

In this section, we describe the *local-minima tree*. First, we define local minima as paths which are invariant under minimization of a cost functional. We then associate an equivalence class to each local minimum, consisting of all paths converging to the same local minimum. Using this equivalence relation, we then construct a local-minima space. To visualize the local-minima space, we finally group local-minima into a tree using the fiber bundle construction [20].

To construct the local-minima tree, we assume to be given the following sets and functions. Let  $(X_f, x_I, x_G)$  be a motion planning problem,  $P$  its path space, and  $c : P \rightarrow \mathbb{R}_{\geq 0}$  be a cost functional on the pathspace. We assume that there exists a path optimization algorithm that we represent as a mapping  $f_c : P \rightarrow P$ , which takes any path and transforms the path into a path having a locally minimal cost. We make no further assumptions about the optimizer, such as that the output optimum is close to the initialization. Instead, our notion of path equivalence will be relative to a any given  $f_c$ . Further, we assume  $X$  to have the structure of an admissible fiber bundle  $X_K \rightarrow X_{K-1} \rightarrow \dots \rightarrow X_0$  with  $X_K = X$ . The fiber bundle comes equipped with lower-dimensional projections  $\pi_K, \dots, \pi_1$ .

##### A. Local-Minima Space

The minimization function  $f_c$  partitions<sup>3</sup> the pathspace. The partition is given by an equivalence relation we call the path equivalence. Given the path-equivalence, we can construct the quotient of the pathspace under path-equivalence. We call this space the local-minima space.

Let us start by defining path-equivalence. If two paths converge, under the optimizer  $f_c$  of the cost  $c$ , to the same path, we say they are path-equivalent. Formally, given two paths  $\mathbf{p}, \mathbf{p}' \in P$ , we say that they are *path-equivalent*, written as  $\mathbf{p} \sim_{f_c} \mathbf{p}'$ , if

$$f_c(\mathbf{p}) = f_c(\mathbf{p}') \quad (3)$$

It is straightforward to check that path-equivalence is an equivalence relation (i.e. reflexive, symmetric, transitive). The optimizer  $f_c$  therefore partitions the pathspace [17].

To better understand this partition, we construct the local-minima space as the quotient-space of all equivalence classes of  $P$  under  $f_c$ , denoted as

$$Q = P / \sim_{f_c} \quad (4)$$

Elements of the space  $Q$  are equivalence classes of paths. We will, however, *represent* each equivalence classes by the path which is invariant under minimization of the cost. We call those paths local minima.

To simplify matters, we will only consider *simple* local minima. A simple local minimum is a local minimum without self-intersections. Simple paths are easier to compute and often capture all important local minima in a problem. However, we note that there are certain pathological cases,

<sup>3</sup>A partition of a set  $X$  is a family of disjoint non-empty sets such that every element of  $X$  is in exactly one such set.

where non-simple paths are required to solve the problem [21].

##### B. Sequential Projections of the Local-Minima Space

To efficiently represent the local-minima space, we propose to sequentially partition the space using the fiber bundle projections. This works as follows: Two distinct local minima of  $Q$  are projected onto a quotient-space  $X_k$  using the mapping  $\pi_k$ . We then consider them to be projection-equivalent, when, under minimization  $f_c$ , they converge to the same path.

More formally, given two local minima  $\mathbf{q}, \mathbf{q}' \in Q$ , we say that they are *projection-equivalent*, written as  $\mathbf{q} \sim_{\{f_c, \pi_k\}} \mathbf{q}'$ , if

$$f_c(\pi_k(\mathbf{q})) = f_c(\pi_k(\mathbf{q}')) \quad (5)$$

Projection-equivalence is again an equivalence relation and therefore partitions the local-minima space. We denote the quotient of  $Q$  under the projection-equivalence as  $Q_{K-1}$ . We then iterate this process for each projection mapping. Thus, given an admissible fiber bundle  $X_K \rightarrow X_{K-1} \rightarrow \dots \rightarrow X_0$ , we construct a sequence of local-minima spaces  $Q_K, \dots, Q_0$  with  $Q_K = Q$ . In other words, the local-minima space  $Q_{k-1}$  is obtained from  $Q_k$  as the quotient-space

$$Q_{k-1} = Q_k / \sim_{\{f_c, \pi_k\}} \quad (6)$$

We will denote an element of  $Q_k$  as a  $k$ -level local minimum.

##### C. Local-Minima Tree

Finally, we use the sequence of local-minima spaces to construct the local-minima tree. The tree consist of all elements of  $Q_0, \dots, Q_K$  as nodes. Two nodes are connected by a directed edge, if the first node is a local minimum  $\mathbf{q}_k$  of  $Q_k$ , the second node is a local minimum  $\mathbf{q}_{k+1}$  of  $Q_{k+1}$ , and we have  $f_c(\pi_{k+1}(\mathbf{q}_{k+1})) = \mathbf{q}_k$ . Additionally, we add one empty-set root node which is connected to every element of  $Q_0$ .

Note that a complete description of the local-minima tree is only possible in trivial cases. In any real-world scenario, we can only hope to visualize certain subsets of the tree.

##### D. Examples

To make the preceding discussion concrete, we visualize the local-minima tree for two examples.

First, we use a free-floating 3-dof planar car with fiber bundle  $SE(2) \rightarrow \mathbb{R}^2$ , which represents the removal of orientation by projection onto a circular disk. The environment is shown in Fig. 2 (c-f) and the fiber bundle is shown in Fig. 2(a). The planning problem is to find a path to go from the green initial configuration to the red goal configuration. We observe that there are four simple local-minima, depending on if the car is going through the top or bottom slit, and going forward or backward. The two top slit paths are projection equivalent and we group them together. The same for the bottom paths. The local-minima tree is then shown in Fig. 2(b).

Second, we use a fixed-based 2-dof manipulator robot with fiber bundle  $S^1 \times \mathbb{R}^1 \rightarrow S^1$  ( $S^1$  is the circle space), which represents the removal of the last link. The environment is shown in Fig. 3 (c-e) (obstacle in grey) with fiber bundle shown in Fig. 3(a). There are three simple local-minima, two going clockwise below (c) and above (d) the obstacle, and one going counterclockwise (e). We group them according to their projection-equivalence as counterclockwise and clockwise, respectively. The local-minima tree is shown in Fig. 3(b)

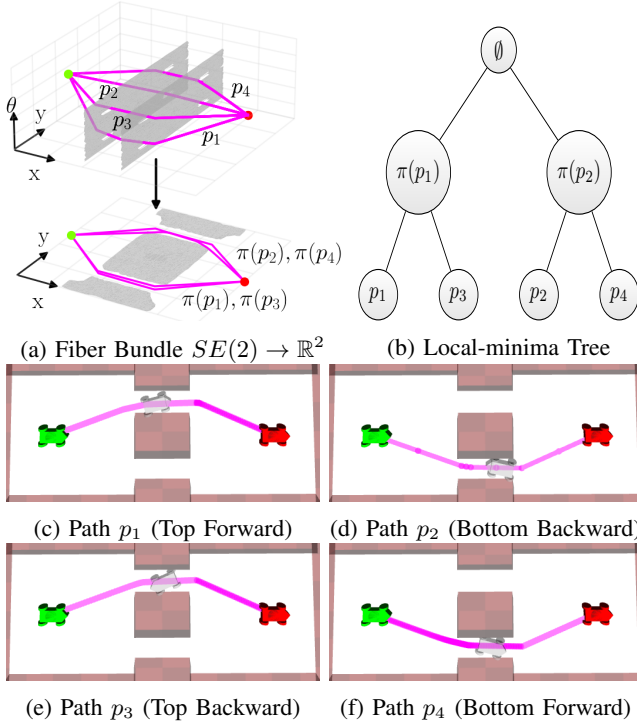


Fig. 2: Car in 2D with configuration space  $SE(2)$ . The planning problem can be decomposed into four parts.

## V. ALGORITHM

To compute the local-minima tree, we develop the *motion planning explorer* (Algorithm 1). The motion planning explorer takes as input a planning problem  $(X_f, x_I, x_G)$ , a minimization method  $f_c$  and a sequence of quotient spaces  $X_1, \dots, X_K$  with  $X_K = X$ . The explorer depends on four parameters, namely  $N \in \mathbb{N}$ , the maximum number of local-minima to display,  $t_{max} \in \mathbb{R}_{>0}$ , the maximum time to sample,  $\delta_S \in \mathbb{R}_{>0}$ , the fraction of space to be visible for the underlying sparse roadmap and  $\epsilon \in \mathbb{R}_{\geq 0}$ , the  $\epsilon$ -neighborhood of a local-minima to sample. Given the input, we return a browsable local-minima tree  $T$ . A user can navigate this tree by clicking on local minima and by collapsing or expanding the minimum, similar to how one navigates a unix directory structure.

Our algorithm consists of an alternation of two phases. In phase one (Line 1.3), a human user can navigate the local-minima tree and select one local minima. In the beginning the user has only one choice, selecting the root node (the

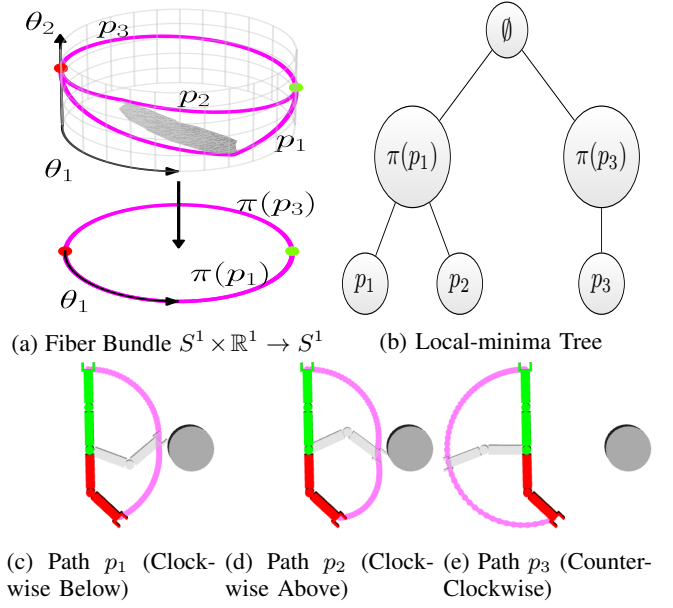


Fig. 3: 2D Manipulator with environment which can be decomposed into three parts. Note that the three shown paths cannot be deformed into each other.

empty-set minimum). In the second phase (Line 1.4), the human user presses a button and the algorithm uses the selected local minimum  $\mathbf{q}_k$  on  $Q_k$  to find all local minima on  $Q_{k+1}$  which, when projected, would be equivalent to  $\mathbf{q}_k$ . For each local minimum we find, we add a directed edge from  $\mathbf{q}_k$  to the local minimum. Note that we construct the local-minima tree in a top-down fashion, which differs from the bottom-up description in Sec. IV. This construction is more computationally efficient, but we might create *spurious local-minima*, which are local minima which do not have any children. In other words, there are no local-minima which, when projected, would be equivalent to the spurious local minimum. This second phase is run for a predetermined maximum timelimit  $t_{max}$ , and can be run multiple times until the user has found sufficiently many local minima.

For phase one of the explorer, we develop a graphical user interface (GUI). The GUI is shown in Fig. 4, where we show the local minima tree (1), the last button pressed (2), the initial configuration (3), the goal configuration (4), and a configuration along a local minimum (environment is hidden to remove distractions). Pressing the button `left` or `right` switches local minima on the same level. Pressing `up` collapses the current local minimum and displays the local minimum on the next lower-dimensional quotient space, which is obtained by projection and subsequent optimization of the current local minimum. Pressing `down` expands the current local minimum. Pressing the button `u` executes the current local minimum path by sending it to the robot and pressing the button `w` starts the search for more local minima.

In the second phase (Algorithm 2), we take the selected local minimum  $\mathbf{q}_k$  on the minimum space  $Q_k$ . We then fix  $\mathbf{q}_k$  as a *path bias* on  $X_k$  (Line 2.2), i.e. whenever we sample

---

**Algorithm 1**

---

**]MotionPlanningExplorer( $x^I, x^G, X_1, \dots, X_K, N, t_{\max}$ )**

---

```

1:  $T = \emptyset$ 
2: while True do ;
3:    $k, \mathbf{q}_k = \text{SELECTLOCALMINIMA}(T)$ 
4:    $\text{UPDATERMINIMATREE}(k, \mathbf{q}_k, T, t_{\max})$ 
5: end while
6: return  $\emptyset$ 

```

---



---

**Algorithm 2** UpdateMinimaTree( $k, \mathbf{q}_{k'}, T, t_{\max}$ )

---

```

1:  $k' = \min(k + 1, K)$ 
2:  $\text{SETLOCALMINIMA}(\mathbf{q}_{k'}, X_{k'})$ 
3: while  $\neg \text{PTC}$  do
4:    $\text{GROWROADMAP}(X_k)$ 
5: end while
6:  $\{q_1, \dots, q_M\} \leftarrow \text{ENUMERATEPATHS}(X_k)$ 
7:  $Q_{\text{new}} \leftarrow \emptyset$ 
8: for each  $\mathbf{q}$  in  $\{q_1, \dots, q_M\}$  do
9:   if  $\neg \text{MINIMAE EXISTS}(\mathbf{q}, Q_{\text{new}})$  then
10:     $Q_{\text{new}} \leftarrow Q_{\text{new}} \cup \mathbf{q}$ 
11:   end if
12:   if  $\text{SIZE}(Q_{\text{new}}) \geq N$  then
13:     break
14:   end if
15: end for
16:  $\text{ADDMINIMATOTREE}(Q_{\text{new}}, T)$ 

```

---



---

**Algorithm 3** MinimaExists( $\mathbf{q}, Q_{\text{new}}$ )

---

```

1: for each  $\mathbf{q}'$  in  $Q_{\text{new}}$  do
2:   if  $\text{ISVISIBLE}((\mathbf{q}, \mathbf{q}'))$  then
3:     return True
4:   end if
5: end for
6: return False

```

---



---

**Algorithm 4** GrowRoadmap( $X_k$ )

---

```

1:  $x_{\text{rand}} \leftarrow \text{SAMPLEFIBER}(\mathbf{G}_{k-1}, \mathbf{q}_{k-1}, F_k)$ 
2:  $x_{\text{near}} \leftarrow \text{NEAREST}(x_{\text{rand}}, \mathbf{G}_k)$ 
3:  $x_{\text{new}} \leftarrow \text{CONNECT}(x_{\text{near}}, x_{\text{rand}}, \mathbf{G}_k)$ 

```

---

a configuration from  $X_k$ , we sample a configuration from  $\mathbf{q}_k$ , and then uniformly perturbate this sample to lie in an  $\epsilon$ -neighborhood of the path. We then sample the space  $X_{k+1}$  (or  $X_K$  if  $k = K$ ) with the path bias on  $X_k$  similar to the Quotient-Space roadMap Planner (QMP) algorithm [21] (Line 2.4). This is detailed in Algorithm 4. First we sample a configuration on the graph  $\mathbf{G}_{k-1}$  biased towards  $\mathbf{q}_{k-1}$ . This configuration indexes a fiber through the inverse mapping  $F_k = \pi_k^{-1}$ . We then sample the fiber, compute the nearest configuration and connect if possible. This is an important step, because we thereby bias sampling towards paths which, when projected onto  $X_k$ , will be projection-equivalent to  $\mathbf{q}_k$ . If the algorithm finds, however, a path not projection-

equivalent to  $\mathbf{q}_k$ , we ignore the path.

The implementation of the roadmap differs from QMP, however, since we maintain two graphs. First, the full roadmap  $G$ , as in the original QMP. Second, we maintain a sparse subgraph  $S$  of  $G$ . Our implementation utilizes previous work from the Sparse Roadmap Spanners (SPARS) algorithm<sup>4</sup> [6]. The sparse subgraph  $S$  utilizes the parameters  $\delta_S$  which determines the maximum visibility radius of a vertex.

After the time  $t_{\max}$  has been reached (or some other Planner Terminate Condition (PTC)), we stop the generation of  $S$ , and enumerate (up to)  $N$  paths on  $S$  (Line 2.6). We generate those  $N$  simple paths by using a depth-first graph search on  $S$ . For each path found, we use the optimization function  $f_c$  to let it converge to the nearest local minimum. We then try to add this path to a set of local minima paths (Line 2.8 to 2.15). The path is added if it is not visible from any path in the set (Line 2.9). We implement the visibility function following the algorithm by [11]. Another option would be to compute a distance between two paths. However, we found this to be unsatisfactory, because two paths could converge to two distinct local minimum, while at the same time being arbitrarily close to each other for some pathspace metric.

Once all simple paths have been enumerated, and the local minima saved, we stop the phase, add all found local minima to the local-minima tree (Line 2.16) and display them to the user in the GUI. Then we return to phase one.

The motion planning explorer has been implemented in C++ and uses the Klampt library [9] for simulation and visualisation, and the Open Motion Planning Library (OMPL) [27] for roadmap computation and fiber bundle projection. The implementation is freely available at [github.com/aorthey/MotionPlanningExplorerGUI](https://github.com/aorthey/MotionPlanningExplorerGUI).

## VI. DEMONSTRATIONS

We demonstrate the motion planning explorer on four realistic and two pathological scenarios. In each scenario, we have used the parameters  $N = 7$  (the maximum amount of visualized paths), the sparsity parameter  $\delta_S = 0.1$  (the fraction of space visible from a vertex). We further set  $\epsilon$  to 0.1 times the measure of the space, and we have adjusted  $t_{\max}$  to be between 1s to 10s. We perform each visualization on a  $4 \times 2.50\text{GHz}$  processor laptop using 7.2 GB Ram and operating system Ubuntu 16.04.

We do not compare to existing methods, because we are not aware of any other algorithm which can (1) visualize local optima for any motion planning problem, (2) let a human user interact with it.

We demonstrate the algorithm on four scenarios. First, a drone in a forest with fiber bundle  $SE(3) \rightarrow \mathbb{R}^3$ , corresponding to a sphere nested inside the drone. The outcome is shown in Fig. 5 (Left). The upper Figure shows seven local minima on the quotient space (magenta). Note that

<sup>4</sup>In particular, we add a vertex to the sparse roadmap whenever the configuration increases visibility, increases connectivity or constitutes a useful cycle.

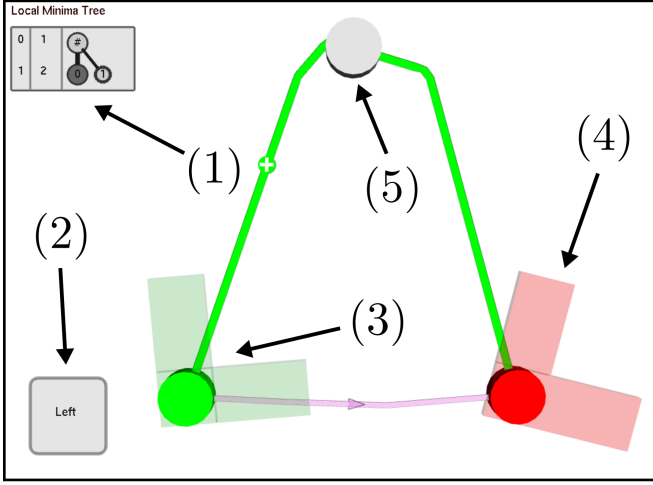


Fig. 4: **Motion Planning Explorer GUI:** (1) local-minima tree depiction. Columns show fiber bundle level, number of nodes on level and nodes of tree, respectively. (2) last button pressed by user. (3) initial (green) configuration on quotient-space (non-transparent disk) and on bundle space (transparent). (4) same for goal (red) configuration. (5) local minima selected by user and highlighted in tree.

the quotient space is topologically trivial, but computing homotopical deformations would be computationally inefficient [11].

The user selects the green path in phase one. We then compute local minima on the configuration space which project onto this path. In this case we find one single local-minima on  $SE(3)$ , which we then execute.

Second, we use a robotic arm (Fig. 5 Middle) in an environment with a large coffee machine which has a visible geometric protrusion. The fiber bundle is  $\mathbb{R}^7 \rightarrow \mathbb{R}^3$ , obtained by removing the first three links of the robotic arm. The explorer finds two local minima on the quotient space which belong to a motion below the protrusion and above the protrusion, respectively. Finally, the user selects the path going above the protrusion, and the explorer finds three local minima which belong to different rotations of the manipulator around its axes.

Third, we use the PR2 robot in a navigation scenario. The fiber bundle is  $SE(2) \times \mathbb{R}^{31} \rightarrow SE(2) \times \mathbb{R}^7 \rightarrow \mathbb{R}^2$ , which corresponds to the removal of arms, and upper torso, respectively. On the lowest-dimensional quotient space, we find three local minima (Fig. 5 Right), which correspond to going left or right around the table, and one going underneath the table. Note that the path underneath the table is spurious (see Sec. V).

In the last scenario, we visualize the flight paths of dubin's airplane [14]. Dubin's airplane is a rigid body in 3D with velocity constraints such that it flies at a constant forward velocity of  $+0.5\text{m s}^{-1}$  and has bounds on the first derivative of yaw and pitch of  $\pm 0.1\text{m s}^{-1}$ . The fiber bundle is  $SE(3) \times \mathbb{R}^6 \rightarrow \mathbb{R}^3$ , which corresponds to the removal of dynamical constraints and orientation. We see that the

Scenario	Time $Q_0$ (s)	Time $Q_{>0}$ (s)	Total Time (s)
Planar Manipulator	0.51	0.82	1.33
Planar Car	1.57	3.16	4.73
Drone in Forest	9.57	0.89	10.46
Robotic Arm	2.03	10.57	12.6
PR2	4.61	292.29	296.9
Dubin's Airplane	2.15	12.34	14.49

TABLE I: Time (s) to generate the local-minima tree in the demonstration cases shown in Video.

algorithm finds two distinct local minima on the quotient space, which corresponds to going through and outside the archway. We then select the local minima going through the archway and the algorithm finds a dynamically feasible path (Fig. 6 Right).

This demonstrates that our method can be extended to dynamical systems, even when shortest path of the geometrical system is neither dynamically feasible nor near to a dynamically feasible path. However, as the demonstration shows, we do not compute a dynamically optimal path, but leverage the optimizer on the quotient space to evaluate path equivalence. Future work should incorporate optimal kinodynamic planners [16].

Finally, we show example runtimes in Table I for each scenario, together with the two examples from Sec. IV. The runtimes show the time to compute the local minima space  $Q_0$  (Column 1), and the time to compute the remaining local minima spaces  $Q_{>0}$  (Column 2) together with their sum (Column 3). Note that those times do not include the interaction by the user, and might differ depending on which minima has been selected.

#### A. Pathological Scenarios

While the motion planning explorer works well on realistic scenarios, it might not work well on pathological cases. To test this, we demonstrate the performance on two scenarios which have been crafted to break the algorithm.

In the first scenario (Fig. 7 Left), we need to move a ball with configuration space  $\mathbb{R}^3$  from an initial (green) to a goal (red) configuration. Between the configurations we place a lattice with openings slightly larger than the radius of the ball. All local minima through the lattice have a neighborhood in pathspace with a vanishingly small measure. Our algorithm, however, rarely detects those minima, but usually finds minima with a higher cost going around the lattice.

In the second scenario (Fig. 7 Right), we place a spherical obstacle between the initial and goal configuration of the ball (As described by Karaman and Frazzoli [13]). The number of local minima is uncountable infinite. Our algorithm finds a small set of local minima but is not able to describe the complete uncountable set.

## VII. CONCLUSION

We introduced the motion planning explorer, an algorithm taking a planning problem as input and computing an local-minima tree. Local minima are defined as paths which are



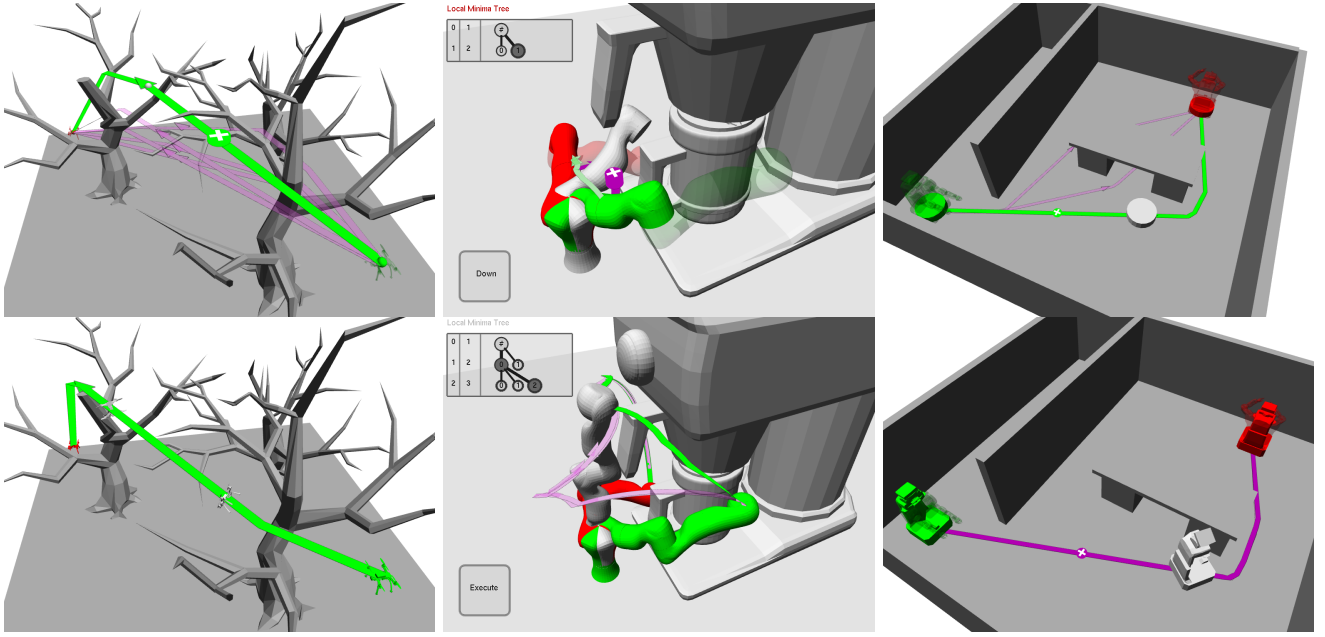


Fig. 5: **Left:** 6-dof Drone **Middle:** 7-dof KUKA LWR **Right:** 34-dof PR2

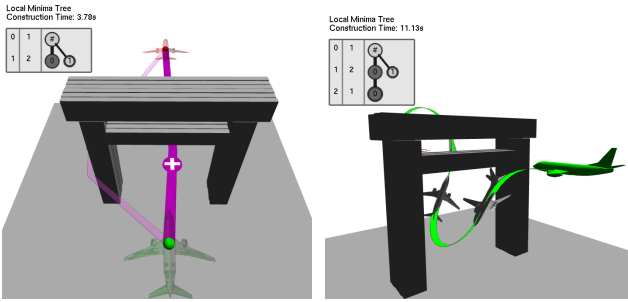


Fig. 6: Dubin's airplane with constant forward velocity of  $0.5\text{m s}^{-1}$  and bounds on first derivative of yaw and pitch of  $\pm 0.1\text{m s}^{-1}$ . The dynamics are modelled as a driftless airplane [22].

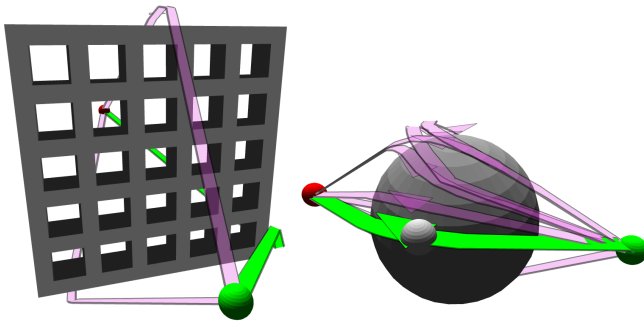


Fig. 7: Limitations: (A) low-cost small-measure local-minima are often ignored in favor of high-cost but large-measure local-minima. (B) Only a countable number of paths is found from an uncountable number of local minima.

invariant under minimization of a cost functional. The local-minima are grouped into a tree, where two paths are grouped together if they are projection-equivalent under a lower-

dimensional fiber bundle projection. We showed that the resulting local-minima tree faithfully captures the structure of many real-world problems.

The implementation of the local-minima tree has, however, three limitations. First, we restrict computation to  $N$  simple paths, which makes the tree non-exhaustive. This could be alleviated by letting a user add additional local-minima and by adding a path enumeration procedure using non-simple paths. Second, the runtime is sometimes prohibitive for real-time application. We believe this could be addressed by specifically tailored hardware [18], parallelization or code optimization. Third, the construction of the tree depends on prespecified lower-dimensional projections. We could remove this dependency by enumerating all projections [20] and use a specific projection only if it will group at least two local minima together.

Most importantly, however, the computation time spent constructing the local-minima tree is negligible compared to having a tool which allows us to visualize, debug and interact with a planning problem.

## VIII. ACKNOWLEDGEMENTS

This paper was supported by the Alexander von Humboldt foundation. We thank Marc Moll and Zachary Kingston for independent code reviews and the website TurboSquid for providing 3D models.

## REFERENCES

- [1] "Black box." [Online]. Available: <https://www.merriam-webster.com/dictionary/black%5Cbox>
- [2] O. B. Bayazit, D. Xie, and N. M. Amato, "Iterative relaxation of constraints: a framework for improving automated motion planning," in *IEEE International Conference on Intelligent Robots and Systems*, 2005, pp. 3433–3440.
- [3] S. Bhattacharya and R. Ghrist, "Path homotopy invariants and their application to optimal trajectory planning," *Annals of Mathematics and Artificial Intelligence*, vol. 84, no. 3-4, pp. 139–160, 2018.

- [4] S. Bhattacharya, M. Likhachev, and V. Kumar, "Topological constraints in search-based robot path planning," *Autonomous Robots*, vol. 33, no. 3, 2012.
- [5] O. Brock and O. Khatib, "Elastic strips: A framework for motion generation in human environments," *International Journal of Robotics Research*, 2002.
- [6] A. Dobson and K. E. Bekris, "Sparse roadmap spanners for asymptotically near-optimal motion planning," *International Journal of Robotics Research*, vol. 33, no. 1, pp. 18–47, 2014.
- [7] M. Farber, "Topology of random linkages," *Algebraic & Geometric Topology*, vol. 8, 2008.
- [8] P. Ferbach and J. Barraquand, "A method of progressive constraints for manipulation planning," *Transactions on Robotics*, vol. 13, no. 4, pp. 473–485, 1997.
- [9] K. Hauser, "Robust contact generation for robot simulation with unstructured meshes," in *International Journal of Robotics Research*. Springer, 2016, pp. 357–373.
- [10] M. Hawasly, F. T. Pokorny, and S. Ramamoorthy, "Multi-scale Activity Estimation with Spatial Abstractions," in *3rd International Conference on Geometric Science of Information*, 2017, pp. 273–281.
- [11] L. Jaillet and T. Siméon, "Path deformation roadmaps: Compact graphs with useful cycles for motion planning," *International Journal of Robotics Research*, 2008.
- [12] L. Janson, E. Schmerling, A. Clark, and M. Pavone, "Fast marching tree: A fast marching sampling-based method for optimal motion planning in many dimensions," *International Journal of Robotics Research*, vol. 34, no. 7, pp. 883–921, 2015.
- [13] S. Karaman and E. Frazzoli, "Sampling-based algorithms for optimal motion planning," *International Journal of Robotics Research*, vol. 30, no. 7, 2011.
- [14] S. M. LaValle, *Planning Algorithms*. Cambridge University Press, 2006.
- [15] J. Lee, *Introduction to topological manifolds*. Springer Science & Business Media, 2010, vol. 202.
- [16] Y. Li, Z. Littlefield, and K. E. Bekris, "Asymptotically optimal sampling-based kinodynamic planning," *International Journal of Robotics Research*, 2016.
- [17] J. Munkres, *Topology*. Pearson, 2000.
- [18] S. Murray, W. Floyd-Jones, Y. Qi, D. J. Sorin, and G. Konidaris, "Robot motion planning on a chip," in *Robotics: Science and Systems*, 2016.
- [19] D. Nieuwenhuisen and M. H. Overmars, "Useful cycles in probabilistic roadmap graphs," in *IEEE International Conference on Robotics and Automation*, vol. 1, 2004, pp. 446–452.
- [20] A. Orthey and M. Toussaint, "Rapidly-exploring quotient-space trees: Motion planning using sequential simplifications," in *International Symposium of Robotics Research*, 2019.
- [21] A. Orthey, A. Escande, and E. Yoshida, "Quotient-space motion planning," *IEEE International Conference on Intelligent Robots and Systems*, 2018.
- [22] A. Orthey, O. Roussel, O. Stasse, and M. Taïx, "Motion planning in irreducible path spaces," *Robotics and Autonomous Systems*, vol. 109, pp. 97–108, 2018.
- [23] F. T. Pokorny, M. Hawasly, and S. Ramamoorthy, "Topological trajectory classification with filtrations of simplicial complexes and persistent homology," *International Journal of Robotics Research*, vol. 35, no. 1-3, pp. 204–223, 2016.
- [24] V. Ranganeni, O. Salzman, and M. Likhachev, "Effective footstep planning for humanoids using homotopy-class guidance," in *Twenty-Eighth International Conference on Automated Planning and Scheduling*, 2018.
- [25] E. Schmitzberger, J.-L. Bouchet, M. Dufaut, D. Wolf, and R. Husson, "Capture of homotopy classes with probabilistic road map," in *IEEE International Conference on Intelligent Robots and Systems*, vol. 3, 2002, pp. 2317–2322.
- [26] S. Smale, "On the topology of algorithms, i," *Journal of Complexity*, vol. 3, pp. 81–89, 1987.
- [27] I. A. Şucan, M. Moll, and L. Kavraki, "The open motion planning library," *Robotics and Automation Magazine*, 2012.
- [28] M. Toussaint and M. Lopes, "Multi-bound tree search for logic-geometric programming in cooperative manipulation domains," in *IEEE International Conference on Robotics and Automation*. IEEE, 2017, pp. 4044–4051.
- [29] M. Zucker, N. Ratliff, A. Dragan, M. Pivtoraiko, M. Klingensmith, C. Dellin, J. A. D. Bagnell, and S. Srinivasa, "CHOMP: Covariant

Hamiltonian Optimization for Motion Planning," *International Journal of Robotics Research*, 2013.